

## Linewidths of the electronic excitation spectra of donors in silicon

C. Jagannath, Z. W. Grabowski, and A. K. Ramdas

*Department of Physics, Purdue University, West Lafayette, Indiana 47907*

(Received 30 September 1980)

The excitation spectra of phosphorus, arsenic, isolated interstitial lithium, and lithium oxygen donors in silicon have been investigated under the high resolution of a Fourier-transform spectrometer. Using a "strain-free" mounting technique, the linewidths are observed to be much narrower than those reported earlier in the literature; the observed linewidths appear to be limited by the "lifetime" effects. The linewidths and shapes of the excitation lines of phosphorus donors in silicon, introduced by the nuclear transmutation of  $^{30}\text{Si}$  into  $^{31}\text{P}$  by the capture of a slow neutron followed by a  $\beta^-$  decay, are studied; the influence of the charged defects produced by neutron irradiation is demonstrated and explained in terms of the electric fields due to charged impurities and defects.

### I. INTRODUCTION

There is continuing interest in the natural width and shape of the line spectra exhibited by carriers bound to impurities in semiconductors and in the factors which lead to the observed linewidths and shapes. The various mechanisms observed and/or proposed in this context are (1) interaction of bound carriers and phonons,<sup>1,2</sup> (2) overlap of the wave functions of bound carriers,<sup>3</sup> (3) random electric fields produced by ionized and neutral impurities causing Stark and quadrupole broadening,<sup>4</sup> and (4) strains resulting from the presence of impurities, both electrically active and inactive.<sup>5</sup> Unusual line broadening can occur due to special circumstances, e.g., in the excitation spectrum of bismuth donors and of gallium acceptors in silicon remarkable broadening of specific lines due to a resonant interaction between the electronic excitation and an optical phonon has been reported and theoretically analyzed.<sup>6-9</sup> Linewidths and shapes of the various lines of the excitation spectrum can be used as probes to study these broadening phenomena. As a basis for such studies it is essential to study the "natural" linewidths of the various lines. Having established the natural linewidths, changes in the width and shape can be correlated to the broadening mechanism present.

In the present paper we report the results of our measurements on the excitation spectra of phosphorus, arsenic, lithium, and lithium-oxygen donors in silicon recorded under the high-resolution accessible with a Fourier-transform spectrometer. We have studied such spectra with carefully characterized host crystals in which the desired dopant has been introduced under well-specified conditions and investigated the influence of charged defects on the linewidths and line shapes.

### II. EXPERIMENTAL PROCEDURE

The Lyman spectra of the Si(P), Si(As), Si(Li), and Si(Li-O) occur in the infrared region between 30 and 60  $\mu\text{m}$ . The large spectral coverage and the high resolution of a Fourier-transform spectrometer are ideal for the present investigation. We have employed a Beckman-RIIC FS-720 spectrometer<sup>10</sup> in which the fixed mirror was moved by 5 cm so as to obtain one-sided interferograms with a maximum path difference of 10 cm. A maximum resolution of 0.025  $\text{cm}^{-1}$  (0.003 meV) was attainable with the spectrometer. We have used a Golay pneumatic cell<sup>11</sup> and a germanium bolometer<sup>12</sup> interchangeably as the detector. The backbone of the data acquisition and processing system is a General Automation<sup>13</sup> SPC-16/40 minicomputer. For experiments in which the data points exceeded 4096, as in the case of high-resolution work ( $\sim 0.06 \text{ cm}^{-1}$ ), the digitized output was punched out on cards and analyzed on a CDC 6500 computer.<sup>14</sup>

The optical cryostat used in the present studies has been described by Fisher *et al.*<sup>15</sup> The sample is attached to a copper tailpiece which is in contact with liquid helium. With the high resolution used for studying the linewidths and line shapes it was found that sample mounting demanded special considerations, especially for samples thinner than  $\sim 1.5 \text{ mm}$ . To avoid the broadening of lines due to the stresses produced in the sample mounting and cooling, a copper tailpiece shown in inset A of Fig. 1 was used. GE 7031 varnish<sup>16</sup> was used at the bottom only. The image of the entrance aperture on the sample was at least 1 cm from the bottom of the sample. This technique produced "strain-free" mounting for samples down to 0.2 mm in thickness.

Group-V donors can be introduced into an otherwise well-characterized host during the crystal growth

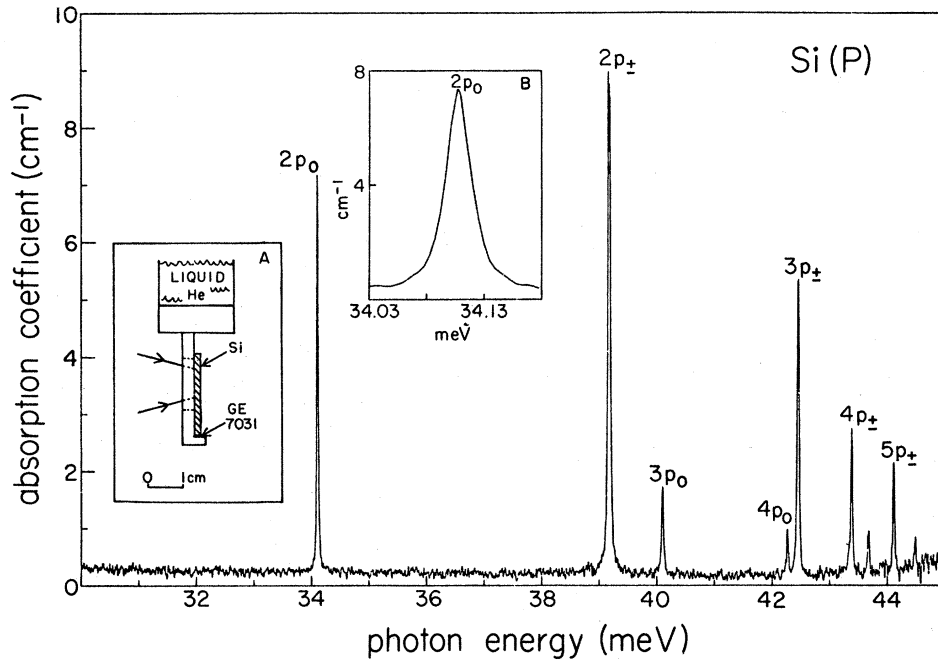


FIG. 1. Excitation spectrum of phosphorus donors in neutron transmutation doped silicon. Liquid helium is used as a coolant. Phosphorus donor concentration,  $n$ ,  $\sim 1.2 \times 10^{14} \text{ cm}^{-3}$ . The instrumental resolution with and without apodization is 0.09 and 0.06  $\text{cm}^{-1}$ , respectively. The  $2p_0$  line with an expanded horizontal scale is shown in the inset. The  $2p_{\pm}$  line has been truncated because, with the thickness of the sample used, the transmission approaches zero at the peak.

in a deliberate and controlled manner, as dopants added to the melt in the Czochralski method or in the form of suitable gaseous components allowed to enter the vacuum chamber in which the crystal is grown by the floating zone technique<sup>17</sup>; we refer to such samples as "conventionally doped." Impurities like lithium can be incorporated into an otherwise

pure host crystal by diffusion followed by quenching.<sup>18</sup> An ingenious technique<sup>19,20</sup> of introducing phosphorus in silicon is based on the nuclear transmutation of  $^{30}\text{Si}$  into  $^{31}\text{P}$  by the capture of a slow neutron followed by a  $\beta^-$  decay; the isotope  $^{30}\text{Si}$  occurs in natural silicon with an abundance of 3.1%. In Table I the various isotopes of silicon and the cross section for thermal neutron capture, in barns, are listed together with the half-life of the end product of the nuclear reaction. We refer to such samples as neutron transmutation doped (NTD).

TABLE I. Neutron transmutation of silicon isotopes.

Natural abundance	Isotope	Cross section $\sigma(n, \gamma)$
97.27%	$^{28}\text{Si}$	$0.08 \pm 0.03b$
4.68%	$^{29}\text{Si}$	$0.28 \pm 0.09b$
3.05%	$^{30}\text{Si}$	$0.11 \pm 0.01b$
100%	$^{31}\text{P}$	$0.20 \pm 0.02b$

$^{28}\text{Si}(n, \gamma)^{29}\text{Si}$
$^{29}\text{Si}(n, \gamma)^{30}\text{Si}$
$^{30}\text{Si}(n, \gamma)^{31}\text{Si} \xrightarrow{2.62 \text{ h}} ^{31}\text{P} + \beta^-$
$^{31}\text{P}(n, \gamma)^{32}\text{P} \xrightarrow{14.3 \text{ d}} ^{32}\text{S} + \beta^-$

### III. EXPERIMENTAL RESULTS AND DISCUSSION

In this section we present the results on the excitation spectra of donors in samples free from charged defects; the liquid-helium temperatures at which the measurements were done result in linewidths free from phonon broadening.

Figure 1 shows the excitation spectrum of phosphorus donors introduced by neutron transmutation<sup>21</sup> in a silicon sample. The silicon sample<sup>22</sup> was exposed to a thermal flux of  $2.5 \times 10^{13}$  neutrons/ $\text{cm}^2 \text{ sec}$  for 7–8 h, yielding a phosphorus concentration of  $\sim 1.2 \times 10^{14} \text{ cm}^{-3}$ . The sample was annealed at 800 °C to remove the damage by the neutron irradiation. A series of sharp excitation lines is observed in

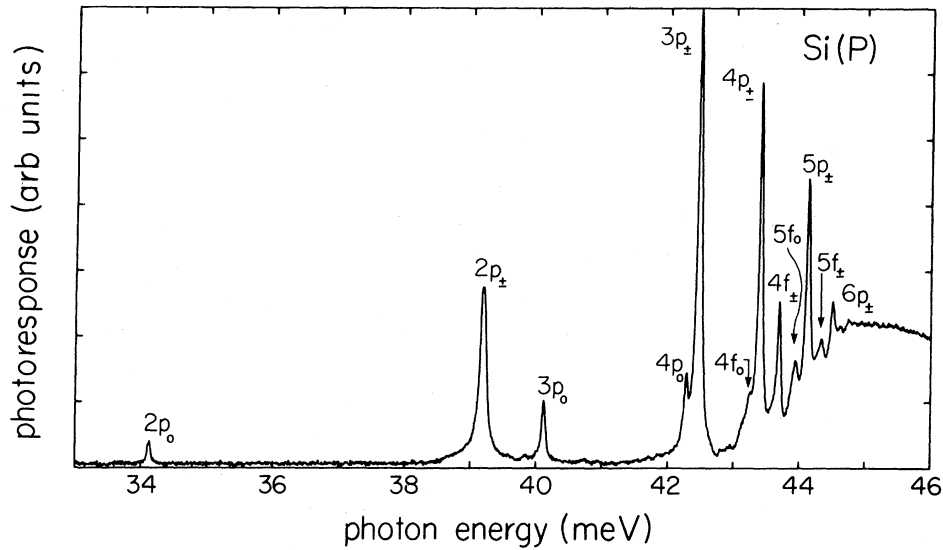


FIG. 2. Photothermal ionization spectrum of phosphorus donors in silicon. Phosphorus donor concentration is estimated to be  $\sim 2 \times 10^{14} \text{ cm}^{-3}$ . Instrumental resolution  $\sim 0.06 \text{ cm}^{-1}$  without apodization.

the range 32 to 45 meV. The occurrence of the spectrum clearly demonstrates the existence of bound states as predicted by the hydrogenic model. The sharp lines are transitions from the  $1s$  ground state to the excited  $p$  states. An extraordinarily sensitive method for the study of the excitation spectra of impurities in semiconductors is the photothermal ionization technique.<sup>23</sup> This is a two step process; the electron is first excited from the ground state to a higher level and then thermally excited into the conduction band. As a result of this process, a photoconductive

peak is recorded, the sample itself serving as the detector. Figure 2 shows the photothermal ionization spectrum of phosphorus donors in silicon. A comparison of Figs. 1 and 2 clearly demonstrates how the intensities of the peaks in the photothermal ionization spectrum reflect the product of the transition probability for the transition to the excited state and the factor controlling the thermal ionization from the excited state to the conduction band; many of the optical transitions close to the conduction band thus appear prominently in Fig. 2. Figure 3 shows the exci-

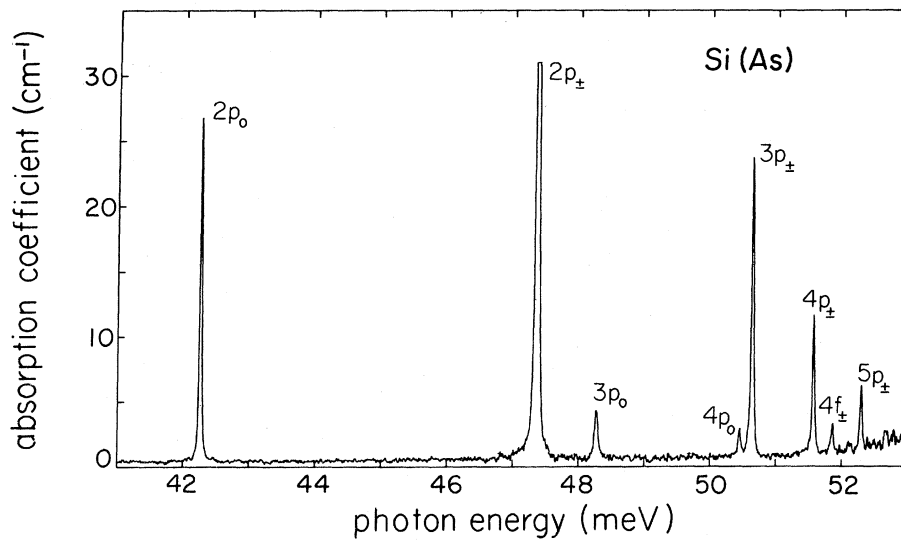


FIG. 3. Excitation spectrum of arsenic donors in silicon. Liquid helium is used as a coolant. Instrumental resolution  $0.06 \text{ cm}^{-1}$  without apodization. Room-temperature resistivity of the sample  $\sim 6 \text{ } \Omega \text{ cm}$  ( $n \sim 7 \times 10^{14} \text{ cm}^{-3}$ ).

tation spectrum of Si(As) where arsenic donors have been introduced into floating zone silicon in a conventional manner. The spacings of the lines in Figs. 1 and 3 are the same although the positions are clearly shifted. This arises due to the  $1s(A_1)$  ground state being depressed below the effective mass position by different amounts in Si(P) and Si(As).<sup>24</sup> The excited  $p$  states are correctly described in the effective mass approximation and the excitation lines in the Lyman spectrum are the  $1s(A_1) \rightarrow np$  transitions.

Following Kohn and Luttinger,<sup>25</sup> a detailed theoretical study of the binding energies of the donor levels for silicon was carried out by Faulkner<sup>26</sup> using the

Ritz method. Table II compares the theoretical calculations of Faulkner with those deduced from the experimentally observed transition energies; they are computed assuming that the theory accurately gives the binding energy of the  $3p_{\pm}$  state as 3.12 meV. It is clear that the theory is remarkably successful in accounting for the spacings of the excitation lines; the  $p$  states can thus be understood on the basis of the effective mass theory.

Apart from the substitutional group-V impurities another striking donor in silicon is lithium. It is well known that lithium enters the silicon lattice interstitially.<sup>27</sup> This is not surprising in view of the small

TABLE II. Binding energies of the energy levels of donors in silicon (meV).

Level	P <sup>a</sup>	As <sup>a</sup>	Sb <sup>b</sup>	Bi <sup>c</sup>	Li <sup>a</sup>	Li-O <sup>a</sup>	Mg <sup>+d</sup>	Mg <sup>d</sup>	Se <sup>e</sup>	Theory <sup>f</sup>
$1s(A_1)$	45.59	53.76	42.74	70.98	$31.24 \pm 0.02$	39.67	256.47	107.50	186.42	31.27
$1s(E)$	32.58 <sup>b,g,h</sup>	31.26 <sup>b,h</sup>	30.47 <sup>b,h</sup>							31.27
$1s(E + T_2)$					33.02	32.00				31.27
			32.89	32.89 <sup>i</sup>					30.92	
$1s(T_2)$	33.89	32.67 <sup>b</sup>							26.22	31.27
			32.91	31.89 <sup>i</sup>					24.02	
$2p_0$	11.48	11.50	11.51	11.44	11.51	11.57	47.84	11.70	11.4	11.51
$2s$		9.11 <sup>j</sup>		8.78 <sup>j</sup>						8.83
$2p_{\pm}$	6.40	6.40	6.38	6.37	6.40	6.40	26.25 26.05	6.38	6.2	6.40
$3p_0$	5.47	5.49	5.50 <sup>k</sup>	5.48	5.49	5.51	22.60	5.55	5.5	5.48
$3s$				4.70						4.75
$3d_0$	3.83 <sup>k</sup> 3.73	3.8 <sup>j</sup>		3.80						3.75
$4p_0$	3.31	3.31	3.33 <sup>k</sup>	3.30	3.32	3.33	13.47	3.33		3.33
$3p_{\pm}$	3.12	3.12	3.12	3.12	3.12	3.12	12.48	3.12	3.12	3.12
$4s$				2.89						2.85
$4f_0$	2.33			2.36						2.33
$4p_{\pm}, 5p_0$	2.19	2.19	2.20 <sup>k</sup>	2.18	2.20	2.20	8.55	2.17		2.19, 2.23
$4f_{\pm}$	1.90	1.90	1.94 <sup>k</sup>	1.91	1.90	1.90				1.89
$5f_0$	1.65		1.71 <sup>k</sup>	1.67	1.64	1.66				1.62
$5p_{\pm}$	1.46	1.46	1.48 <sup>k</sup>	1.46	1.47	1.47		1.45		1.44
$5f_{\pm}$	1.26			...	1.25	1.29				1.27
$6p_{\pm}$	1.09	1.07 <sup>b</sup>	1.10 <sup>k</sup>	1.08	1.07	1.09				1.04

<sup>a</sup>Present work. The binding energies given for Li-O are for the  $A$  series; the binding energy for  $1s(E + T_2)$  for that series is from Ref. 18.

<sup>b</sup>R. L. Aggarwal and A. K. Ramdas, Phys. Rev. A **140**, 1246 (1965); R. L. Aggarwal and A. K. Ramdas (unpublished).

<sup>c</sup>Reference 7.

<sup>d</sup>L. T. Ho and A. K. Ramdas, Phys. Rev. B **5**, 462 (1972); the binding energies for the excited states of  $Mg^+$  have to be divided by 4 in order to compare them with theory.

<sup>e</sup>W. E. Krag and H. J. Zeiger, Phys. Rev. Lett. **8**, 485 (1962).

<sup>f</sup>Reference 26.

<sup>g</sup>G. B. Wright and A. Mooradian, Phys. Rev. Lett. **18**, 608 (1967).

<sup>h</sup>K. L. Jain, S. Lai, and M. V. Klein, Phys. Rev. B **13**, 5448 (1976).

<sup>i</sup>W. E. Krag, W. H. Kleiner, and H. J. Zeiger, in *Proceedings of the Tenth International Conference on the Physics of Semiconductors, Cambridge, Massachusetts, 1970*, edited by S. P. Keller, J. C. Hensel, and F. Stern (U.S. AEC Division of Technical Information, Washington, D.C., 1970), p. 271.

<sup>j</sup>B. Pajot, J. Kauppinen, and R. Anttila, Solid State Commun. **31**, 759 (1979).

<sup>k</sup>W. H. Kleiner and W. E. Krag, Phys. Rev. Lett. **25**, 1490 (1970).

ionic radius and the very large diffusion coefficient of the lithium donors in the host lattice; for example, at 800 °C the diffusion coefficient of phosphorus in silicon is about  $10^8$  times smaller than that of lithium.<sup>28</sup> Another remarkable property which has attracted considerable attention is the ability of lithium to complex with other chemical impurities simultaneously present in the host.<sup>29,30</sup> The presence of oxygen in silicon leads to the formation of lithium-oxygen complexes which behave electrically as donors.<sup>18</sup>

Figure 4 shows the spectrum of lithium introduced into a high-purity floating zone silicon sample.<sup>31</sup> Identifying the lowest line at 21.50 meV as the  $1s \rightarrow 2p_0$  transition, all the other lines can be assigned according to the final state labels given in the figure. Once again, the spacings agree in an excellent manner with those of group-V donors as can be seen in Table II. The relative intensities of the excitation lines in Si(Li) bear a striking resemblance to those of group-V donors in Si. The particularly close agreement of the ionization energy of lithium (33.02 meV) with the theoretical value of Faulkner (31.27 meV) is remarkable. This strongly suggests that the lowest ground state is effective-mass-like. Figure 5 shows the excitation spectrum of lithium donors at a slightly elevated temperature, estimated to be  $\sim 20$  K. This reveals the existence of a line  $1.76 \pm 0.04$  meV below the line labeled  $2p_{\pm}$ . Another line similarly displaced from the transition labeled  $3p_{\pm}$  can also be seen. These lines arise due to transitions from the upper ground state. Polarization studies<sup>18</sup> of the various transitions using uniaxial stress as a perturbation identify the lines seen in Fig. 4 as those arising from the fivefold degenerate,  $1s(E + T_2)$ , lower ground

state. The upper ground state can be identified as a  $1s(A_1)$  state. The interstitial nature of the lithium impurity seems to be the underlying cause for this "inverted" arrangement for the ground state in comparison to that observed for group-V donors. The electron paramagnetic resonance experiments by Watkins and Ham<sup>32</sup> confirm that interstitial lithium donors in silicon have a degenerate  $1s(E + T_2)$  ground state.

Lithium diffused into high-resistivity crucible grown silicon forms donor complexes with the oxygen which enters the silicon from the quartz crucible during crystal growth.<sup>29</sup> The excitation spectrum of lithium introduced in crucible-grown (Czochralski) silicon is shown in Fig. 6. The most prominent series, series *A*, has an ionization energy of 39.67 meV. Other series, labeled *C*, *D*, and *F* can also be clearly identified in Fig. 6. It has been shown by Gilmer *et al.*<sup>33</sup> that the relative intensities of the different series are a function of the annealing history of the sample. Another interesting feature in Fig. 6 is the presence of the  $2p_{\pm}$  line of phosphorus which is evidently present in the silicon into which lithium was diffused.

In Fig. 4 the presence of the  $2p_0$  and  $2p_{\pm}$  line of the *A* series of Li-O complexes indicates that there is some dispersed oxygen even in the float zone silicon used. On doping with lithium a so-called high-purity silicon sample<sup>34</sup> both the isolated lithium and the lithium-oxygen donor transitions were observed simultaneously. In Figs. 7 and 8 different spectral regions of the measurement are shown; the spectrum was recorded at a resolution of  $0.06 \text{ cm}^{-1}$ . From the intensity of the  $2p_0$  line it is estimated that the con-

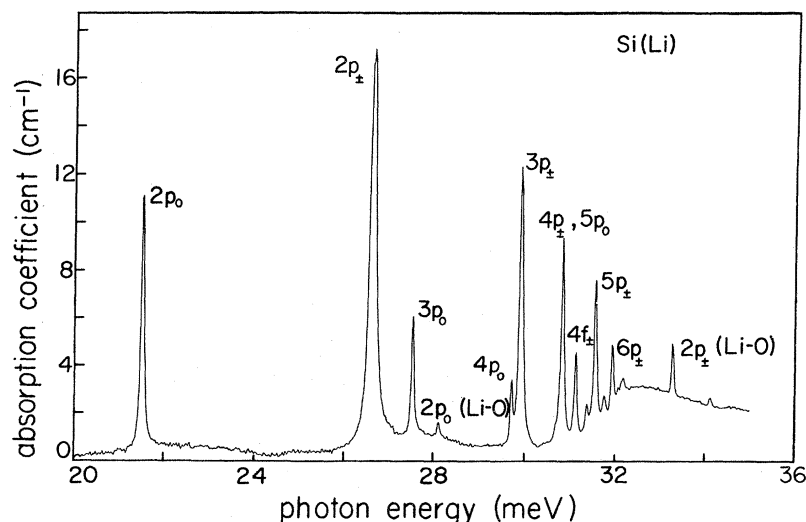


FIG. 4. Excitation spectrum of lithium donors introduced into a high-purity float zone silicon sample (Ref. 31). Lithium donor concentration  $\sim 1.1 \times 10^{15} \text{ cm}^{-3}$ . Liquid helium used as a coolant. Instrumental resolution  $\sim 0.28 \text{ cm}^{-1}$ .

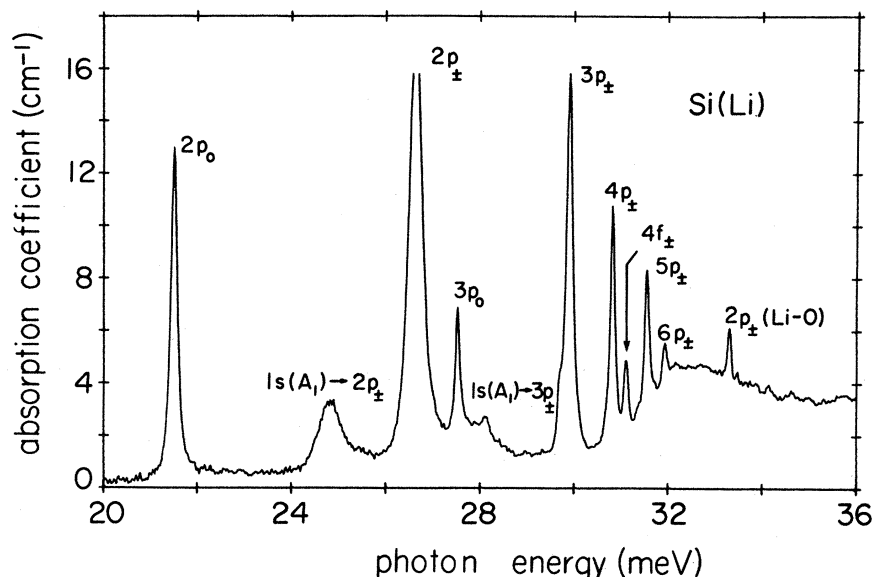


FIG. 5. Excitation spectrum of lithium donors in silicon at a temperature estimated to be  $\sim 20$  K. The transitions labeled  $1s(A_1) \rightarrow 2p_{\pm}, 3p_{\pm}$  correspond to transitions from the upper ground state.

centration of Li and Li-O donors is  $\sim 2 \times 10^{14}$  and  $\sim 3 \times 10^{14} \text{ cm}^{-3}$ , respectively. The simultaneous presence of both isolated lithium and lithium oxygen complexes in the same sample can be visualized as follows: the lithium enters the lattice, first seeks out the dispersed oxygen to form lithium-oxygen complexes and then the excess lithium occupies interstitial positions. This technique of "decorating" the dispersed oxygen with lithium and using the excitation spectrum of the Li-O complexes is clearly very

sensitive in the estimation of very low oxygen concentrations in Si whereas the  $9 \mu\text{m}$  vibrational band of oxygen<sup>35,36</sup> requires concentrations of oxygen in excess of  $10^{16} \text{ cm}^{-3}$ , provided measurements are made at liquid-helium temperature.<sup>37</sup>

Another interesting feature in Fig. 8 is the appearance of the  $2p_{\pm}, 3p_{\pm}$  lines of phosphorus. From the intensity of the  $2p_{\pm}$  line of phosphorus the concentration of phosphorus donors is estimated to be about  $10^{13} \text{ cm}^{-3}$ . The original sample, before doping it with

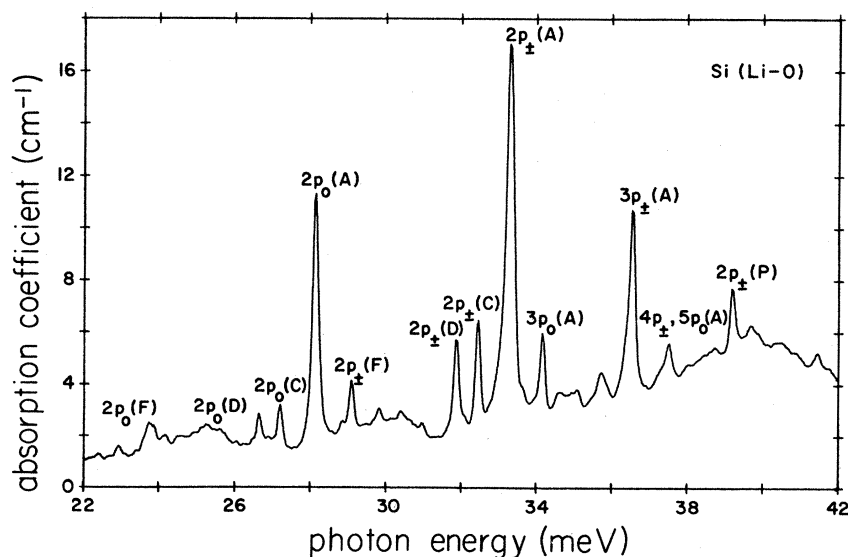


FIG. 6. Excitation spectrum of Li-O donor complexes in silicon. Concentration of donors is  $\sim 1 \times 10^{15} \text{ cm}^{-3}$ . Liquid helium used as a coolant. The transitions are labeled following the nomenclature in Ref. 33. The line labeled  $2p_{\pm}(P)$  is due to residual phosphorus in the sample.

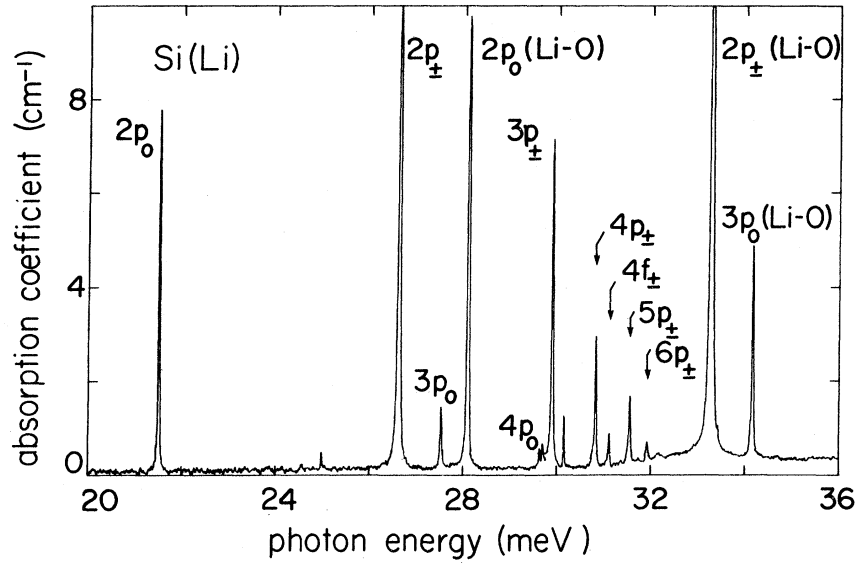


FIG. 7. Excitation spectra of isolated Li donors and Li-O donor complexes in silicon. The transitions corresponding to  $1s(A_1) \rightarrow np$  for Li-O complexes are labeled "Li-O" in parentheses. The concentration of Li and Li-O is estimated to be  $\sim 2 \times 10^{14}$  and  $\sim 3 \times 10^{14} \text{ cm}^{-3}$ , respectively. Liquid helium used as a coolant. The instrumental resolution is 0.09 and  $0.06 \text{ cm}^{-1}$  with and without apodization, respectively.

lithium, is *n* type with a resistivity of  $\sim 6000 \Omega \text{ cm}$ , indicating a net donor concentration of  $\sim 10^{12} \text{ cm}^{-3}$ . The phosphorus concentration of  $\sim 10^{13} \text{ cm}^{-3}$  as estimated from Fig. 8 can be explained by assuming that in the original sample, phosphorus is compensated by some acceptor impurities so that the net donor concentration is  $\sim 10^{12} \text{ cm}^{-3}$ . On introducing lithium into silicon it will deionize and expose *all* the com-

pensated phosphorus donors present since it is shallower.

It is well known that the observed line shape is the convolution of the true line shape with the instrumental function. In a Fourier-transform spectrometer the instrumental function, with no apodization, is given by  $A \text{ sinc}[2\pi L(\nu - \nu_0)]$ , where  $L$  is the optical path difference and the line is centered at  $\nu = \nu_0$ . Us-

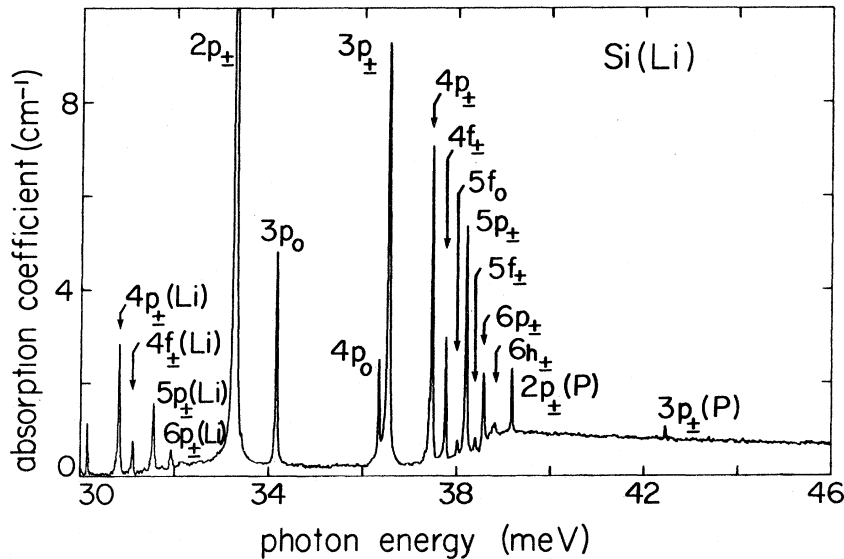


FIG. 8. Excitation spectra of Li donors and Li-O donor complexes in the range 30–46 meV. The Li transitions are labeled "Li" in parentheses. This figure is an extension of Fig. 7. Transitions due to the residual phosphorus in the sample have been identified with "P" in parentheses; the concentration of P is estimated to be  $\sim 10^{13} \text{ cm}^{-3}$ .

TABLE III. Half-widths,  $W_{1/2}$  (meV), of the  $2p_0$ ,  $2p_{\pm}$ , and  $3p_{\pm}$  lines of the excitation spectra of donors in silicon. "Conventional" denotes doping during crystal growth by means of the dopant added to the melt.

Donor	Method of doping	Concentration ( $\text{cm}^{-3}$ )	$W_{1/2}$		
			$2p_0$	$2p_{\pm}$	$3p_{\pm}$
Si(P)	Conventional	$2 \times 10^{14}$	0.026	...	0.033
	Conventional	$4 \times 10^{15}$	0.03	...	0.05
	NTD	$1.2 \times 10^{14}$	0.021	0.027	0.030
		$2 \times 10^{15}$	0.025	...	0.028
Si(As)	Conventional	$7 \times 10^{14}$	0.024	...	0.028
Si(Li)	Diffusion	$2 \times 10^{14}$	0.018	0.025	0.023
Si(Li-O)	Diffusion	$3 \times 10^{14}$	0.025	...	0.023

ing such an instrumental function it can be shown that for both Lorentzian and Gaussian profiles the increase in the full width at half maxima,  $W_{1/2}$ , of the true line function due to the instrumental function is negligible when the observed  $W_{1/2}$  is at least twice as large as the instrumental half-width. In Table III the  $W_{1/2}$  of the spectral lines are tabulated for various donors. The  $W_{1/2}$  of the  $2p_0$  and  $3p_{\pm}$  lines of the excitation spectrum of phosphorus donors introduced in silicon by neutron transmutation shown in Fig. 1 was measured to be 0.021 and 0.030 meV, respectively. The error estimated for these values is  $\sim \pm 0.002$  meV. The  $W_{1/2}$  of the  $2p_{\pm}$  was measured to be  $\sim 0.027$  meV. The  $W_{1/2}$  for the  $2p_0$  and  $3p_{\pm}$  lines

for arsenic donors were obtained from the spectrum shown in Fig. 3; these values, 0.024 and 0.028 meV, respectively, are in excellent agreement with the linewidths of the phosphorus donor spectrum. The corresponding values of the linewidths for the lithium and lithium-oxygen donor complex (series A) are also in close agreement with the above values. Figure 9 shows the excitation spectrum of a sample in which the dopant is introduced during crystal growth, i.e., a conventionally doped sample, with a phosphorus concentration estimated as  $\sim 2 \times 10^{14} \text{ cm}^{-3}$ . The  $W_{1/2}$  for the  $2p_0$  and  $3p_{\pm}$  lines was measured to be 0.026 and 0.033 meV, respectively.

At this stage it is useful to review the contributions

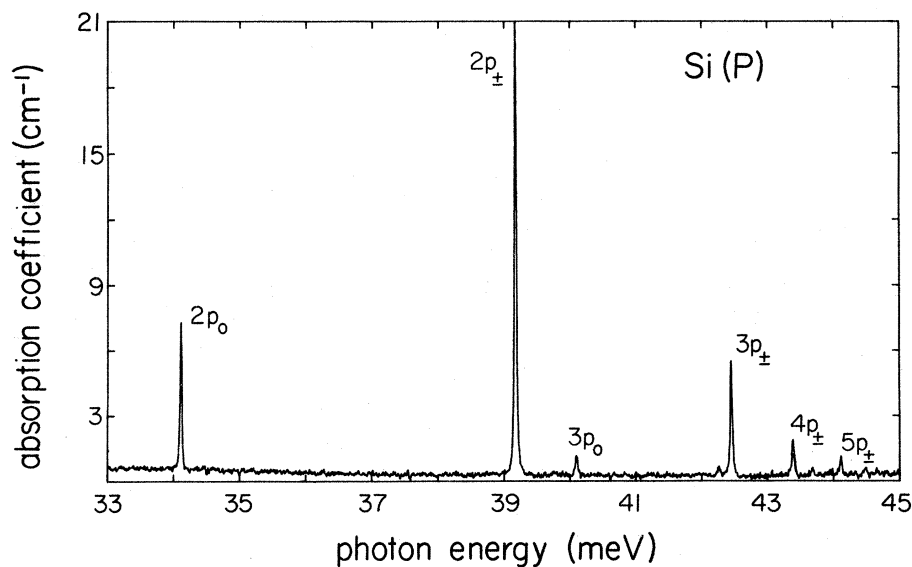


FIG. 9. Excitation spectrum of phosphorus donors in silicon. The dopant is added to the melt during crystal growth. Donor concentration is estimated to be  $\sim 2 \times 10^{14} \text{ cm}^{-3}$ . Liquid helium is used as a coolant. The instrumental resolution, without apodization, is  $\sim 0.06 \text{ cm}^{-1}$ .



to the half-width arising from various broadening mechanisms.

(i) *Interaction of bound carriers and phonons.* The interaction between the lattice vibration, phonons, and the electronic excitation levels leads to broadening of the spectral lines. Lax and Burstein<sup>1</sup> proposed that the interaction of the donor electron and acoustic phonons in the crystal produces a broadening of the  $1s$ ,  $2p$ , . . . levels, the broadening of the  $1s$  ground state accounting for about 90% of the broadening. On the basis of their calculations they predicted that the widths of the excitation lines at 0 K are about 3.6 meV. Using the simple Lorentz broadening approach Sampson and Margenau<sup>38</sup> calculated a low-temperature width of  $\sim 1.6$  meV. These values are larger by about 2 orders of magnitude than the observed linewidths of the donor lines, which are about 0.02 meV. It was pointed out by Kane<sup>2</sup> that the linewidths reported in earlier studies may be entirely instrumental. He suggested that due to the weakness of the electron-phonon interaction in silicon the broadening, free from instrumental effects, arises from a "lifetime effect" due to a transition to a lower state with the emission of a phonon. At  $T = 0$  K he estimated such linewidths to be  $\sim 0.05$  meV. Later, Barrie and Nishikawa<sup>39</sup> confirmed that for a weak electron-phonon interaction, the observed linewidths do arise from a "lifetime effect" and that the process discussed by Lax and Burstein,<sup>1</sup> where the emission or absorption of phonons gives rise to line broadening, only contributes a broad, weak background on which the peak is superimposed. Numerical estimates<sup>39</sup> of the zero-phonon "lifetime broadening" and the one-phonon process indicate that for the  $1s \rightarrow 2p_0$  transition at 0 K the height of the peak for the zero-phonon process is about  $10^3$  times larger than that for the one-phonon process while the full width at half maximum for the one-phonon process is  $\sim 10^2$  times larger than that for the zero-phonon process. In the light of these considerations the measured half width at 0 K arises from the broadening caused by the "lifetime effect." It would be interesting to study the shape of the line close to the base as a function of temperature with a signal-to-noise ratio of better than  $10^3$ .

Taking into account the zero-phonon "lifetime" broadening the linewidths estimated<sup>39</sup> for the  $2p_0$ ,  $2p_{\pm}$ , and  $3p_{\pm}$  lines are less than 0.02, 0.01, and about 0.01 meV, respectively. The characteristic temperature above which the linewidth begins to increase as a function of temperature is greater than 35 K for donors in Si. Thus, at the temperature at which the measurements presented in this paper were made, the effect of temperature can be neglected. Hence the observed linewidths would then reflect the "lifetime broadening."

Resonant interaction between phonons and impurity states has been reported to cause anomalous

broadening of certain excitation lines of gallium acceptors, Si(Ga),<sup>6,8</sup> and bismuth donors, Si(Bi),<sup>6,7</sup> in silicon. The chemical shift of the ground state place the excitation spectra of these impurities in the energy range of the optical phonons of the host; the interaction of line 2 of the gallium acceptor in silicon with the zone center optical phonon ( $\hbar\omega_0 = 64.8$  meV) gives rise to two mixed states. On applying uniaxial stress, the stress-induced components can be tuned out of resonance, with a resultant decrease in the resonant interaction and the consequent sharpening of the excitation lines. The  $2p_0$  line of bismuth donors in silicon was observed to have a width eight times larger than that of the other prominent lines. This has also been interpreted<sup>6,7</sup> as due to an interaction between the donor electron and the optical phonons of the energy of the  $2p_0$  transition and with wave vectors approximately in the  $\langle 110 \rangle$  direction. When uniaxial stress was used to "switch off" the interaction, sharp lines corresponding to  $1s(A_1) \rightarrow 2p_0(-)$  and  $1s(A_1) \rightarrow 2p_0(+)$  were observed;  $2p_0(-)$  and  $2p_0(+)$  originate due to the regrouping of the conduction band minima along  $\langle 100 \rangle$ .

(ii) *Electric field broadening.* Consider an electron bound to a shallow impurity. The potential energy due to the interaction of the charge carrier with all ionized impurities in the crystal,  $V(\vec{r})$ , evaluated at a point  $\vec{r}$  near the neutral donor can be written as<sup>40</sup>

$$V(r) = \sum_i \frac{e_i}{\kappa |\vec{R}_i - \vec{r}|} \\ = 4\pi \sum_i \frac{e_i}{R_i \kappa} \sum_{l=0}^{\infty} \sum_{m=-l}^l \frac{1}{(2l+1)} \left( \frac{r}{R_i} \right)^l \\ \times Y_{lm}^*(\theta_i, \phi_i) Y_{lm}(\theta, \phi) , \quad (1)$$

where  $e_i$  denotes the charge on the  $i$ th impurity ion,  $R_i$ ,  $\theta_i$ ,  $\phi_i$  its position in spherical coordinates, and  $r$ ,  $\theta$ ,  $\phi$  are the spherical coordinates of  $\vec{r}$ . For  $l=0$  Eq. (1) reduces to  $\sum_i e_i/\kappa R_i$  which is the potential evaluated at the donor center  $\vec{r}=0$ . This term shifts all the levels of the neutral donor up or down by the same amount and therefore leaves the transition energies unchanged.

The  $l=1$  terms reduce to  $-\vec{E}(0) \cdot \vec{r}$  where  $\vec{E}(0)$  is the electric field associated with the potential  $V(r)$  also evaluated at the donor center,  $\vec{r}=0$ . Physically this term produces the Stark effect. For weak electric fields the general formula for bound-state energy levels with quantum numbers  $n$ ,  $m$ ,  $n_1$ , and  $n_2$  is<sup>41</sup>

$$\mathcal{E} = -\frac{e^2}{2a_0 n^2} + \frac{3}{2} n(n_1 - n_2) e E a_0 \\ - \frac{E^2 n^4}{16} a_0^3 [17n^2 - 3(n_1 - n_2)^2 - 9m^2 + 19] \\ + \dots , \quad (2)$$

where  $n$  is the principal quantum number and  $m$  is the magnetic quantum number for the component of the orbital angular momentum along the electric field direction,  $a_0$  is the effective Bohr radius, and  $n_1$  and  $n_2$  are integers greater than or equal to zero which obey

$$n = n_1 + n_2 + |m| + 1 \quad (3)$$

In Eq. (2) the second term, proportional to the electric field, is the linear Stark term; the term proportional to  $E^2$  leads to the quadratic Stark shift. These perturbations introduce shifts in infinitely sharp transitions. In the case of donors and acceptors we are always sampling large numbers of them and, in general, the electric fields vary from donor to donor according to a more or less random spatial distribution of charged impurities producing these fields. The shift in the energy levels due to the Stark effect will vary from one donor to another. Thus the net absorption spectrum, observed in the infrared, is a superposition of a large number of sharp absorption lines centered at different frequencies. This leads to a broadening of the transition and the peak position and shape of the absorption line will then reflect the statistical distribution of the electric fields. To estimate the magnitude of the broadening resulting from the Stark effect we can define an average electric field  $\bar{E}$  created by an ion at the donor site to be

$$\bar{E} \approx \frac{e}{\kappa \bar{r}^2} \approx \frac{e}{\kappa} (N_i)^{2/3}, \quad (4)$$

where  $\bar{r}$  is the mean distance between the ions and  $N_i$  is their concentration. Thus for a simple hydrogenic system the ratio of the linear to the quadratic Stark effect is  $\approx 10^{-2}/(N_i a_0^3)^{2/3}$  for the  $3p$  orbit; even for  $N_i \approx 10^{16} \text{ cm}^{-3}$  this ratio is greater than one. However, donors in silicon are not simple hydrogenic systems in that the levels with the same  $n$  quantum number and different azimuthal quantum number,  $l$ , are not degenerate. Hence we do not expect significant linear Stark broadening of the  $2p, 3p, \dots$  levels. As can be seen from Eq. (2) the quadratic Stark effect, for a given electric field, shifts the line to the lower energy side; with a random spatial distribution of charges the line shape would be asymmetric producing a tail towards the lower energy side.

The third term in the multipole expansion [Eq. (1)], the quadrupole term, can be shown to contain terms that are linear in the electric field gradients.<sup>4,42</sup> The broadening due to this effect has been estimated<sup>5</sup> to be of the order of  $(e^2 a_0^2 / \kappa) N_i$ ; this becomes comparable to the broadening expected due to quadratic Stark broadening,<sup>5</sup> which is  $\sim (e^2 a_0^3 / \kappa) N_i^{4/3}$ , when the concentration of charged defects is about  $10^{15} \text{ cm}^{-3}$ .

(iii) *Concentration broadening.* On increasing the concentration of impurities the resulting overlap of the wave functions gives rise to a broadening of the

various energy levels. Baltensperger's<sup>43</sup> calculations of the  $1s, 2s, 2p$  bands for a lattice of hydrogenlike impurities show that the broadening of the "hydrogenic" lines becomes important when

$$r_s \approx 6na_0, \quad (5)$$

where  $n$  is the principal quantum number of the level,  $a_0$  is the effective Bohr radius of the bound carrier in a crystal with dielectric constant  $\kappa$ , and  $r_s$  is defined by

$$\left(\frac{4}{3}\pi\right)r_s^3 = 1/N_i, \quad (6)$$

$N_i$  being the impurity concentration. As we shall show below the half-width of the  $2p_0$  line does not change when the donor concentration is increased from  $1.2 \times 10^{14} \text{ cm}^{-3}$  (Fig. 1) to  $2 \times 10^{15} \text{ cm}^{-3}$  (Fig. 10) indicating that the broadening due to the overlap of wave functions, concentration broadening, does not contribute to the observed linewidth up to at least  $2 \times 10^{15} \text{ cm}^{-3}$  donor atoms. Experimental data of Newman<sup>3</sup> on the line spectra of acceptors in silicon demonstrated that the lines begin to broaden when the acceptor concentration is  $\sim 10^{16} \text{ cm}^{-3}$ . This is in close agreement with the theoretical value obtained from Eq. (5). However, this does not agree with the data obtained by Colbow<sup>44</sup> which showed that concentration broadening starts below  $1.2 \times 10^{15} \text{ cm}^{-3}$  for boron acceptors in silicon; this disagreement with Baltensperger's theory<sup>43</sup> was explained by considering a random distribution of impurities as opposed to a regular spacing of impurities in Baltensperger's calculations. The discrepancy between the data of Newman<sup>3</sup> and Colbow<sup>44</sup> was attributed by the latter to the neglect of instrumental broadening by the former.

(iv) *Other broadening mechanisms.* Besides the donors and acceptors that are present in a semiconductor, some electrically inactive impurities (EII), i.e., impurities which do not give rise to any level in the energy gap can also be present. For example, in floating zone silicon, oxygen and carbon, both of which are electrically inactive impurities, typically occur<sup>7</sup> with concentrations between  $10^{15}$  and  $5 \times 10^{16} \text{ cm}^{-3}$ . The presence of these impurities can cause line broadening. The various mechanisms considered in this context are<sup>5,45</sup> (a) the random strain due to the presence of the impurity resulting in a broadening which is estimated to be  $\sim e^2 a'^2 N_{\text{EII}}$  where  $a'$  is the lattice parameter and  $N_{\text{EII}}$  is the concentration of the electrically inactive impurities, (b) the local potential of the EII which perturbs the quantum state of the electron or hole, and (c) Stark broadening due to the multipole moments associated with the EII. In silicon, with  $N_{\text{EII}} \approx 10^{16} \text{ cm}^{-3}$ , the broadening expected from (a) and (b) is  $\sim 0.005 \text{ meV}$ . The Stark broadening (c) is an order of magnitude smaller.

The presence of dislocations in a crystal can also result in the broadening of the donor lines. These

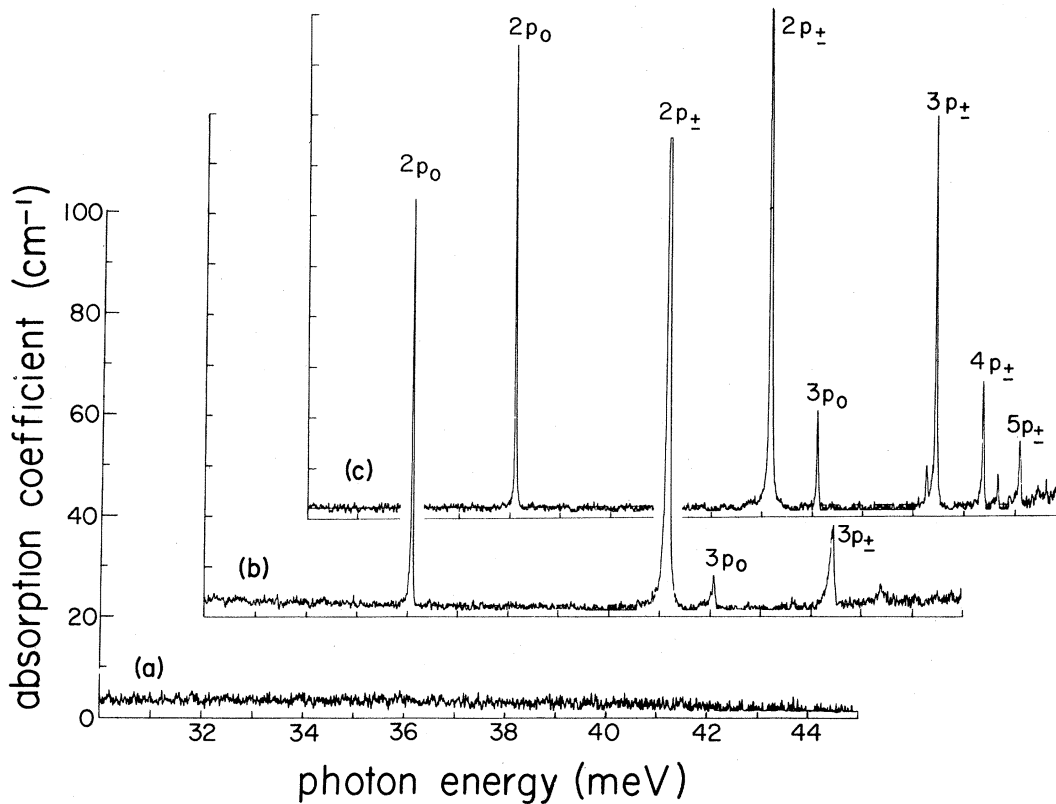


FIG. 10. Annealing of defects produced during the NTD process. The concentration of phosphorus generated is  $\sim 2 \times 10^{15} \text{ cm}^{-3}$ . (a) Before annealing. (b) After annealing for 2 h at  $650^\circ \text{C}$ . (c) After further annealing for 1 h at  $800^\circ \text{C}$ . The spectra were recorded using liquid helium as a coolant. The  $2p_{\pm}$  line has been truncated because, with the thickness of the sample used, the transmission approaches zero at the peak. The instrumental resolution is  $0.06 \text{ cm}^{-1}$  without apodization.

dislocations are expected to give rise to internal strains with magnitude given by<sup>46</sup>  $\sim n^{1/2} \times 10^{-8}$  where  $n$  is the number of dislocation lines per  $\text{cm}^2$ . The shifts in the conduction band minima and hence the broadening of the excited states which follow them are  $\sim n^{1/2} \times 10^{-7} \text{ eV} = n^{1/2} \times 10^{-4} \text{ meV}$ . From the half-widths reported we estimate that the samples used in the present investigation have less than  $10^4$  dislocation lines per  $\text{cm}^2$ . This is consistent with the fact that, with the present state of art of silicon crystal growth, typical dislocation densities observed<sup>47</sup> for float zone silicon are  $10^4$  to  $10^6 \text{ cm}^{-2}$  and  $10^3$  to  $10^4 \text{ cm}^{-2}$  for crucible-grown silicon.

In order to study the influence of the various broadening mechanisms discussed above it is essential to establish the minimum linewidth characteristic of a pure crystal and low temperatures. Thus one must clearly start with well-characterized samples. In this context it is important to estimate the concentration of charged impurities present even in a "pure" sample as a result of unavoidable compensation. As was estimated above, the concentration of charges present in the so-called hyperpure silicon sample as a

result of compensation of phosphorus donors with some acceptor impurities is  $\sim 10^{13} \text{ cm}^{-3}$ . The contribution to the linewidths due to the electric field produced by these compensated impurities is estimated to be less than  $4 \times 10^{-4} \text{ meV}$ . Using the technique of neutron transmutation doping, phosphorus donors with a concentration of  $\sim 2 \times 10^{15} \text{ cm}^{-3}$  were generated in such a silicon sample. From Table III it can be seen that  $W_{1/2}$  for  $2p_0$  and  $3p_{\pm}$  lines are 0.025 and 0.028 meV, respectively, two orders of magnitude larger than the estimated  $W_{1/2}$  due to the electric fields produced by charged impurities with a concentration of  $\sim 10^{13} \text{ cm}^{-3}$ . Thus contribution to the linewidths reported in Table III arising from electric field broadening due to ionized impurities can be neglected. Also, in view of the low temperatures at which the spectra were recorded, phonon broadening is unimportant. Thus the observed  $W_{1/2}$  can be attributed to the "lifetime broadening" discussed earlier. Indeed, the values in Table III are consistent with the estimates of Barrie and Nishikawa<sup>39</sup> quoted earlier.

The effect of charged defects on the linewidths and line shapes of the excitation spectrum of donors in

silicon can be conveniently studied using neutron transmutation doped silicon. Prior to any annealing there is considerable radiation damage produced by the fast neutron component of the neutron flux and the displacement of the phosphorus produced by the neutron transmutation process. It is well known<sup>19,48</sup> that neutron irradiation of silicon produces defects which are effective in trapping carriers and that such defects exhibit a characteristic annealing behavior. Figure 10(a) shows the spectrum of a sample<sup>37</sup> irradiated with a neutron flux of  $1.1 \times 10^{14}$  neutrons/cm<sup>2</sup> sec for 30.6 h. The phosphorus added to the sample is estimated to be  $2 \times 10^{15}$  cm<sup>-3</sup>. The ratio of fast to slow neutrons being 1:10, we expect  $\sim 10^{20}$  cm<sup>-3</sup> defects to be produced by the fast neutrons.<sup>48,49</sup> It is clear that the presence of these defects has compensated all the phosphorus donors and consequently the excitation spectrum is not seen. The sample was then annealed in an atmosphere of flowing helium for 2 h at 650°C. Figure 10(b) shows the spectrum after this annealing. The  $2p_0$ ,  $2p_{\pm}$ ,  $3p_0$ , and  $3p_{\pm}$  lines are clearly observed in the spectrum whereas the  $4p_{\pm}$  and  $5p_{\pm}$  lines cannot be separated from the background. The  $2p_0$  line has a  $W_{1/2}$  of  $\sim 0.025$  meV whereas the  $3p_0$  and  $3p_{\pm}$  lines are broad and asymmetric. An explanation for this broadening is presented below. Figure 10(c) shows the spectrum after the sample was further annealed for 1 h at 800°C. The  $3p_0$  and  $3p_{\pm}$  lines became narrower and the  $4p_{\pm}$  and  $5p_{\pm}$  lines could now be clearly distinguished from the background. Within experimental errors, the intensity and  $W_{1/2}$  of the  $2p_0$  line remained the same after the first anneal, indicating that the same number of donors are responsible for the transitions in Figs. 10(b) and 10(c). Figure 11 compares the  $3p_{\pm}$  line after the two anneals.

The broadening of the  $3p_{\pm}$  line observed in Fig. 10(b) can be attributed to the effect of charged defects on the energy levels. The quadratic Stark broadening and the quadrupole broadening have been estimated<sup>5</sup> to be of the order of  $(e^2 a_{\delta}^3 / \kappa) N_i^{4/3}$  and  $(e^2 a_{\delta}^2 / \kappa) N_i$ , respectively. The quadratic Stark broadening affects the line asymmetrically producing a tail towards the lower energy side.<sup>4,5</sup> From Fig. 11(b) we obtain for the  $3p_{\pm}$  line a  $W_{1/2}$  of 0.1 meV. Charged defects having a concentration of  $\sim 10^{15}$  cm<sup>-3</sup> can account for this broadening and the line shape. Due to the difference in the radii of  $2p$  and  $3p$  orbits, the effect of Stark and quadrupole broadening on the  $2p_0$  line is approximately five times smaller than that on the  $3p_{\pm}$  line. This is in qualitative agreement with Fig. 10(b). Since the  $4p$  and  $5p$  orbits are larger than the  $3p$  orbit, the Stark and quadrupole broadening are even larger and estimated to be  $\sim 0.5$  meV for the  $4p_{\pm}$  and  $5p_{\pm}$  lines. As can be seen from Fig. 10(c) the absorption coefficient at the peak of the  $4p_{\pm}$  line is  $\sim 25$  cm<sup>-1</sup> and the  $W_{1/2} \sim 0.025$  meV. Since the same number of

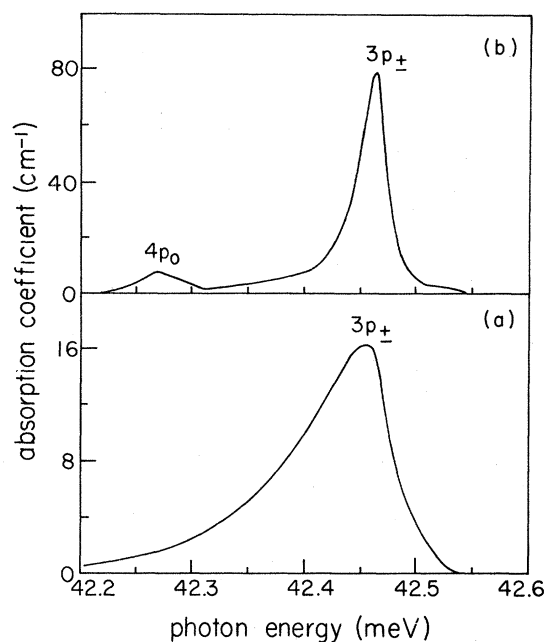


FIG. 11. Comparison of the  $3p_{\pm}$  line during successive annealings. (a) First annealing: annealed at 650°C for 2 h. (b) Second annealing: annealed at 650°C for 2 h and 800°C for 1 h. The spectra were recorded using liquid helium as coolant.

donors contribute to the spectrum in Figs. 10(b) and 10(c), the  $4p_{\pm}$  lines would have been identical in both cases had there been no broadening. If the  $W_{1/2}$  of the  $4p_{\pm}$  line is increased from 0.025 to 0.2 meV, i.e., by a factor of 8, the absorption coefficient at the peak should decrease by about the same factor. This would then make it difficult to separate the  $4p_{\pm}$  line from the background and hence its absence in Fig. 10(b) can be understood.

An ingenious method of introducing controlled quantities of charged impurities in silicon is the introduction of phosphorus by neutron transmutation into a  $p$ -type sample. If the amount of phosphorus introduced is greater than the acceptors already present, the excitation spectrum of phosphorus donors in the presence of a known number of charged impurities produced by compensation can be studied. Figure 12(a) shows the excitation spectrum of one such sample before annealing. Phosphorus was generated by neutron transmutation doping in a silicon sample in which  $\sim 1.5 \times 10^{15}$  cm<sup>-3</sup> boron acceptors were present. The concentration of phosphorus introduced is  $\sim 2.45 \times 10^{15}$  cm<sup>-3</sup>. Thus one expects  $\sim 1 \times 10^{15}$  cm<sup>-3</sup> neutral phosphorus donors to be present in an environment which has  $3 \times 10^{15}$  cm<sup>-3</sup> charged impurities. Of course, before any annealing, the presence of defects due to radiation damage compensates the phosphorus donors entirely and consequently the

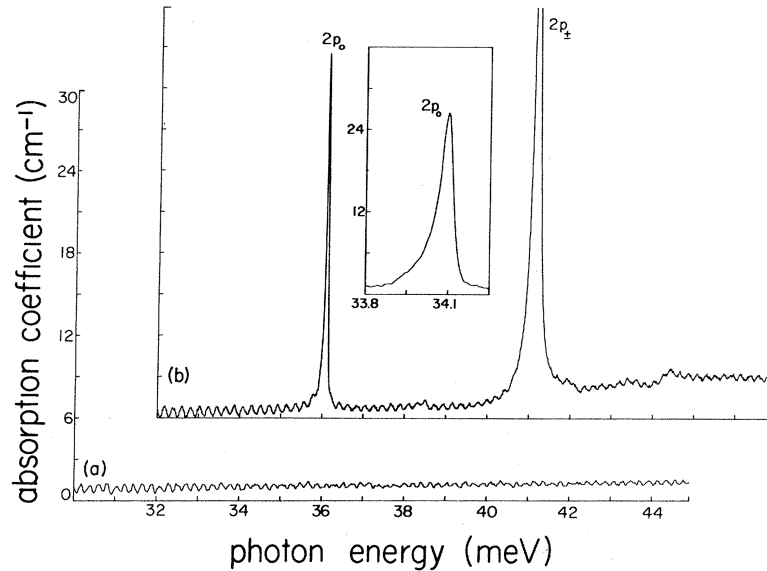


FIG. 12. Excitation spectra of  $2.45 \times 10^{15} \text{ cm}^{-3}$  phosphorus donors introduced by neutron transmutation doping in a silicon sample with  $\sim 1.5 \times 10^{15} \text{ cm}^{-3}$  boron acceptors. (a) Before annealing. (b) After annealing for 2 h at  $800^\circ\text{C}$ . The inset shows the  $2p_0$  line on an expanded horizontal scale. The spectra were recorded using liquid helium as coolant. The "channel spectra" arises due to an insufficient wedge on the sample.

characteristic phosphorus spectrum is not seen. Figure 12(b) shows the spectrum of the sample after the  $800^\circ\text{C}$  annealing for 2 h in an atmosphere of flowing helium. Only the  $2p_0$  and  $2p_{\pm}$  lines can now be seen. Further, they exhibit a pronounced asymmetric tail towards the lower energy region; the inset in Fig. 12(b) clearly shows this asymmetry for the  $2p_0$  line. On annealing further at  $800^\circ\text{C}$  for 2 h the  $W_{1/2}$  of

the lines do not change appreciably. The lines are still asymmetric although they are more symmetric than after the first annealing as can be seen in Fig. 13. A possible explanation for the decrease in the asymmetry without an appreciable decrease in  $W_{1/2}$  is that the second annealing reduces the number of charged impurities. Since the quadratic Stark broadening is  $\propto N_i^{4/3}$  whereas the quadrupole

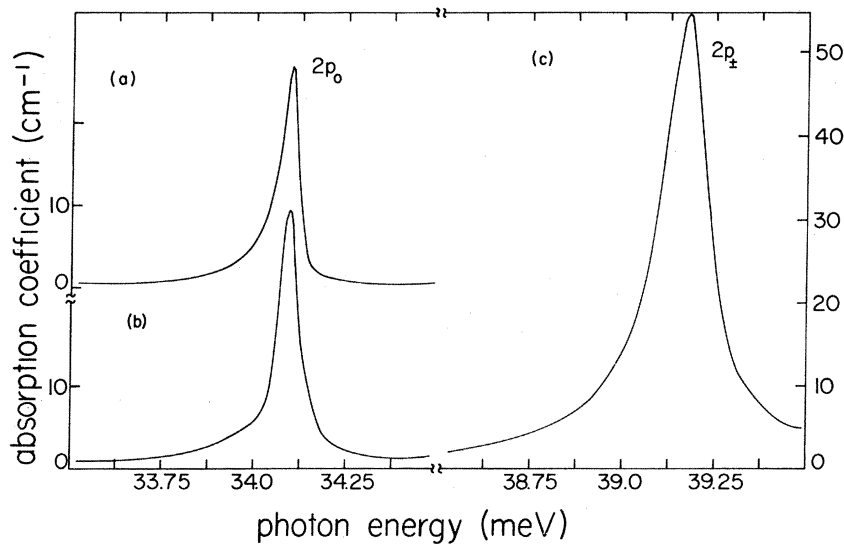


FIG. 13.  $2p_0$  and  $2p_{\pm}$  lines during successive annealings of the NTD sample used in Fig. 12. (a)  $2p_0$  after annealing for 2 h at  $800^\circ\text{C}$ . (b)  $2p_0$  after annealing at  $800^\circ\text{C}$  for 4 h. (c)  $2p_{\pm}$  after annealing at  $800^\circ\text{C}$  for 4 h.

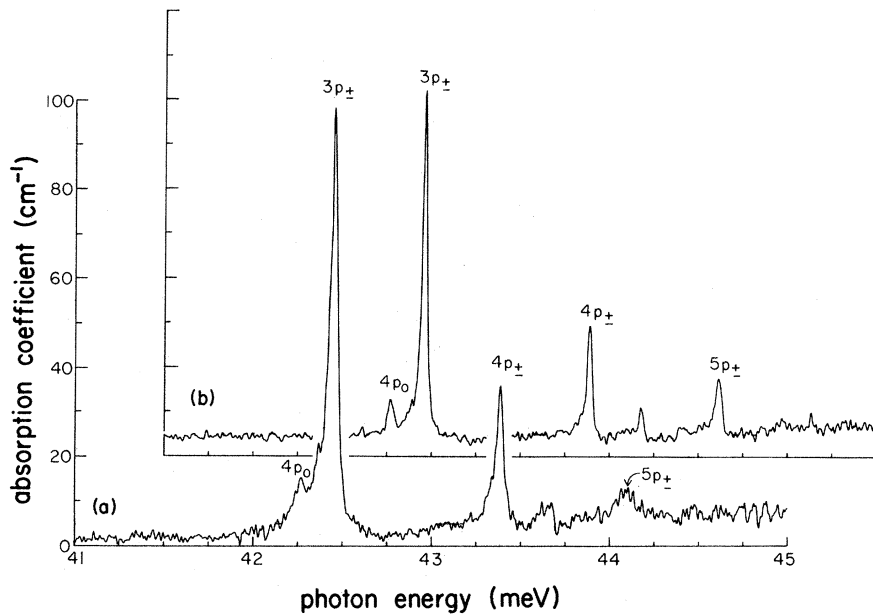


FIG. 14. Comparison of excitation spectra of phosphorus introduced in silicon during crystal growth (conventional doping) and neutron transmutation doping. (a) Conventionally doped silicon with a donor concentration of  $\sim 4 \times 10^{15} \text{ cm}^{-3}$ . (b) Neutron transmutation doped silicon with a donor concentration of  $\sim 2 \times 10^{15} \text{ cm}^{-3}$ .

broadening is  $\propto N_i$ , we expect the quadratic Stark broadening to decrease faster than the quadrupole broadening with decreasing  $N_i$ ; the asymmetry of the line is associated with the quadratic Stark broadening. The  $W_{1/2}$  for the  $2p_0$  and  $2p_{\pm}$  are  $\sim 0.06$  and  $0.15$  meV, respectively, significantly larger than the values quoted in Table III. Thus we note that a concentration of charged defects  $\sim 3 \times 10^{15} \text{ cm}^{-3}$  is sufficient to

produce observable quadratic Stark broadening of the  $2p$  lines and to wipe out the  $3p$  and higher lying lines.

In Fig. 14(a) the excitation spectrum of a conventionally doped sample having a phosphorus concentration  $\sim 4 \times 10^{15} \text{ cm}^{-3}$  is shown. For comparison, we show in Fig. 14(b) the spectrum of a sample with  $2 \times 10^{15}$  phosphorus donors generated by neutron transmutation doping. As can be seen in Fig. 14(a),

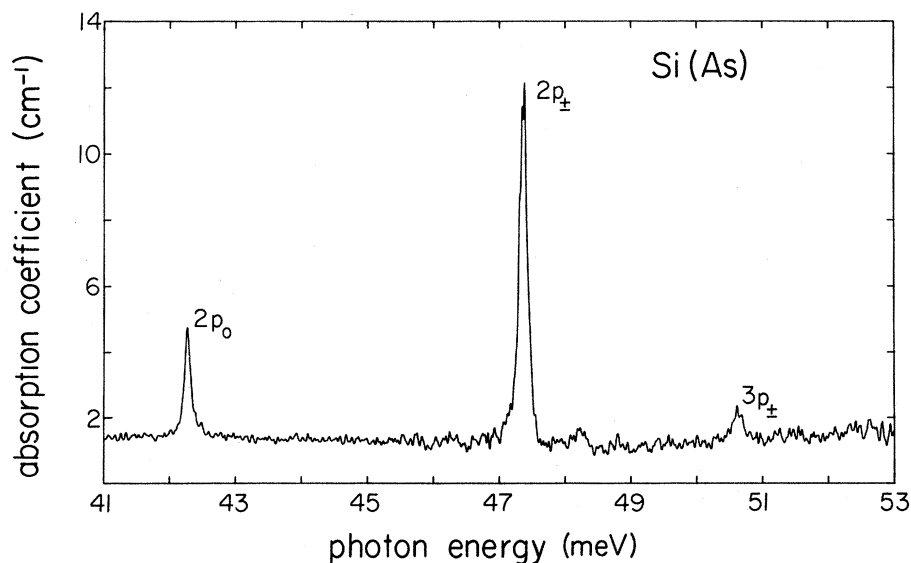


FIG. 15. Excitation spectrum of arsenic donors in silicon with a donor concentration of  $2 \times 10^{14} \text{ cm}^{-3}$ . Liquid helium is used as a coolant.

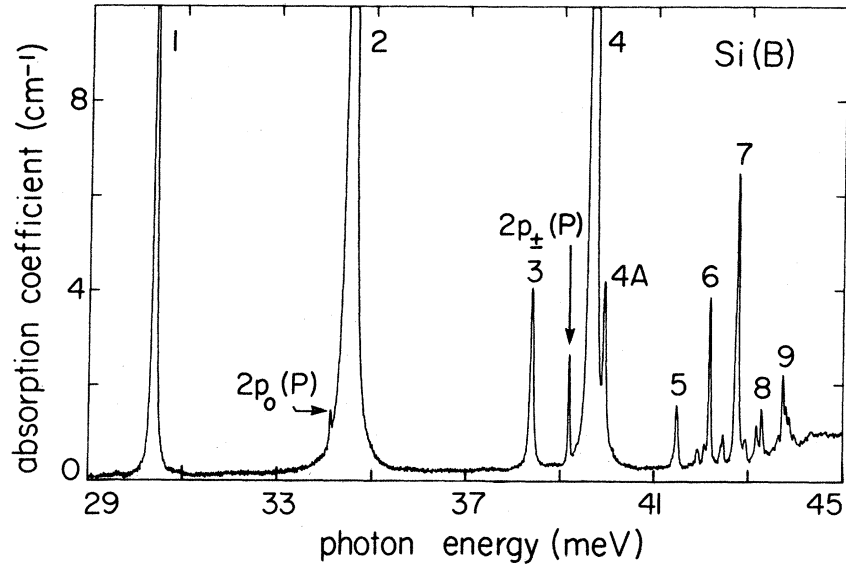


FIG. 16. Excitation spectrum of boron acceptors in silicon. Concentration of acceptors is  $8.5 \times 10^{14} \text{ cm}^{-3}$ . The Si(P) lines are labeled "P" in parentheses. Lines 1, 2, 4 are truncated because, with the thickness of the sample used, the transmission approaches zero at the peak. Liquid helium used as coolant.

the  $5p_{\pm}$  line is rather broad with a  $W_{1/2}$  estimated to be  $\sim 0.15 \text{ meV}$ . Such a broadening can be produced by the presence of  $\sim 4 \times 10^{14} \text{ cm}^{-3}$  ionized impurities. Also the  $3p_{\pm}$  line exhibits pronounced asymmetry with a  $W_{1/2} \sim 0.05 \text{ meV}$ . An interesting illustration of the broadening of lines due to defects introduced

during the crystal growth is shown in Fig. 15. This figure shows the spectrum of arsenic donors, the donor concentration being  $2 \times 10^{14} \text{ cm}^{-3}$ . The absence of lines beyond  $3p_{\pm}$  is a striking feature in this spectrum; also the lines are rather broad. The  $W_{1/2}$  of the  $2p_0$  line is estimated to be  $\sim 0.1 \text{ meV}$ , a factor

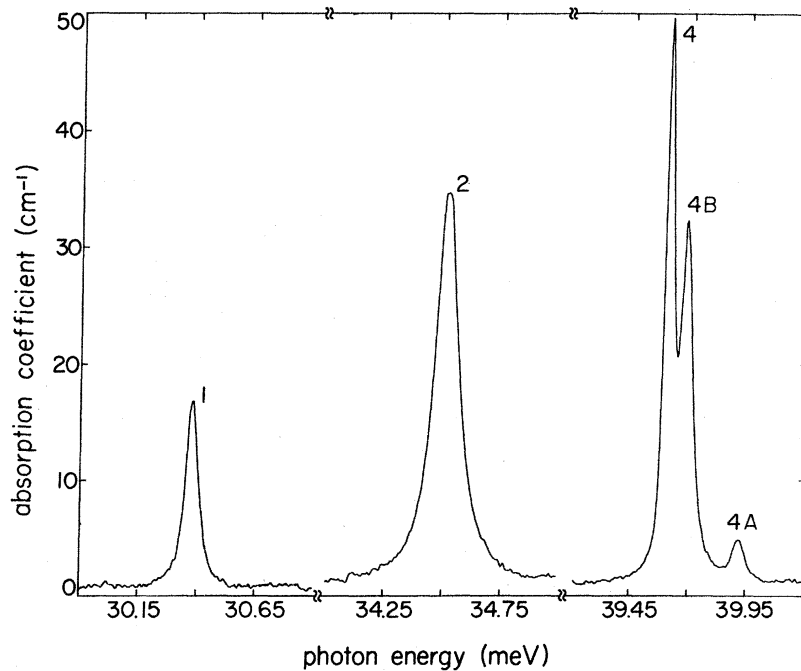


FIG. 17. Lines 1, 2, 4, 4A, of Si(B) shown on an expanded horizontal scale. The sample used is the same as that in Fig. 16 but with reduced thickness. Liquid helium used as coolant.

of 5 larger than the values reported in Table III. The defects responsible for these broad lines could be vacancies, interstitials, dislocations formed during the growth, and other ionized or unionized impurities. Annealing the sample at 800 °C for 2 h in an atmosphere of flowing helium did not, however, change the linewidth.

The present study has demonstrated the effect on the line shapes and widths caused by charged defects even at dilute concentrations. It is of interest to extend such studies to the onset of concentration broadening and establish impurity banding effects.<sup>3,50</sup> Also such linewidth and line shape studies on acceptors should yield interesting information. Our preliminary investigation of the excitation spectrum of boron acceptor in silicon indicates that the various lines do not have the same  $W_{1/2}$ . For example, Fig. 16 shows the excitation spectrum of  $8.5 \times 10^{14} \text{ cm}^{-3}$  boron acceptors in silicon. Besides the expected boron lines we also see the  $2p_0$  and  $2p_{\pm}$  lines of Si(P). These occur because in the spectrometer radiation with energy larger than the band gap of silicon falls on the sample and some of the residual phosphorus gets deionized as a result of charge exchange between the acceptors and donors.<sup>51</sup> When a black polyethylene filter was placed before the sample to block the shorter wavelengths, these phosphorus lines disappeared. From the measurements shown in Figs. 16 and 17 we obtain  $W_{1/2}$ 's of 0.059, 0.105, 0.063, 0.037, 0.061, 0.066, and 0.038 meV for lines 1, 2, 3, 4, 4B, 4A, and 6, respectively.<sup>52</sup> The  $W_{1/2}$  of the  $2p_{\pm}$  line of Si(P) seen in the same spectrum is 0.03 meV. The variation in  $W_{1/2}$  of the various lines of Si(B) are clearly of further interest.

#### IV. CONCLUDING REMARKS

In the present investigation we established what appear to be the true linewidths of the excitation lines in the Lyman spectra of the shallow donors in Si. In view of the importance of this information a further study with a significantly higher resolution is clearly of interest. In the work reported in the present paper the influence of charged defects on linewidths and line shapes has been unambiguously demonstrated. In this connection we wish to draw attention to the report of Nisida *et al.*<sup>53</sup> who have studied the effects of electron irradiation on the donor spectra in germanium; in this short note they showed the preferential disappearance of excitation lines corresponding to

transitions to higher orbits.

We have not observed the effect on linewidths due to the electrically inactive oxygen impurities in crucible-grown silicon, presumably due to its insufficient concentration. In this connection the work of Artjemenko *et al.*<sup>45</sup> is of particular significance; these authors observed splittings in the gallium excitation lines in Ge in the presence of a large substitutional barium in its immediate vicinity. Such investigations in the donor spectra would be of great interest, e.g., the influence of the sizes of two donor species like Bi and Li simultaneously present in Si could demonstrate such effects.

There has always been a strong interest in the effects arising from overlap of wave functions as the donor concentration is increased; starting with the formation of molecular species which are analogs of  $\text{H}_2$  molecule, band formation is a phenomenon of basic interest. The investigations of Newman<sup>3</sup> on the excitation spectra of acceptors in Si, of Imatake<sup>54</sup> on donors in Ge, and of Carter *et al.*<sup>55</sup> on donors in Si and CdTe are of particular interest in this context. The electronic Raman spectra of donor impurities involving the ground-state multiplet in the concentration range where the metal-insulator transition occurs have been reported for Si by Jain *et al.*<sup>56</sup> and for Ge by Doehler *et al.*<sup>57</sup> Capizzi *et al.*<sup>50</sup> have recently reported the spectra of Si(P) in the concentration range of  $2 \times 10^{16}$  to  $2 \times 10^{17} \text{ cm}^{-3}$  where they found evidence for the formation of donor-pair bonds. It would be worthwhile to extend our measurements covering the concentration range from the very dilute to the onset of the metal-insulator transition. Photothermal ionization technique should prove particularly useful in this connection. Such studies would be simplified when carried out under very high uniaxial stress with compressive force along [001] since only the conduction band valleys along [001] and  $[00\bar{1}]$  will be involved in the description of the impurity states.

#### ACKNOWLEDGMENTS

We wish to record our indebtedness to Dr. J. M. Meese, Research Reactor Facility, University of Missouri, for his generous help in neutron irradiations. Our thanks are due to him and Professor Sergio Rodriguez for stimulating discussions and to J. W. Cross for help in some of the measurements. This work has been supported by the National Science Foundation Grant No. DMR 77-27248 and by the NSF-MRL Program No. DMR 77-23798.



- <sup>1</sup>M. Lax and E. Burstein, *Phys. Rev.* **100**, 592 (1955).
- <sup>2</sup>E. O. Kane, *Phys. Rev.* **119**, 40 (1960).
- <sup>3</sup>R. Newman, *Phys. Rev.* **103**, 103 (1956).
- <sup>4</sup>D. M. Larsen, *Phys. Rev. B* **13**, 1681 (1976).
- <sup>5</sup>S. M. Kogan and T. M. Lifshits, *Phys. Status Solidi (a)* **39**, 11 (1977).
- <sup>6</sup>A. Onton, P. Fisher, and A. K. Ramdas, *Phys. Rev. Lett.* **19**, 781 (1967); A. Onton, P. Fisher, and A. K. Ramdas, *Phys. Rev.* **163**, 686 (1967).
- <sup>7</sup>N. R. Butler, P. Fisher, and A. K. Ramdas, *Phys. Rev. B* **12**, 3200 (1975).
- <sup>8</sup>H. R. Chandrasekhar, A. K. Ramdas, and S. Rodriguez, *Phys. Rev. B* **14**, 2417 (1976).
- <sup>9</sup>S. Rodriguez and T. D. Schultz, *Phys. Rev.* **178**, 1252 (1969).
- <sup>10</sup>Beckman Instruments, Inc., 2500 Harbor Blvd., Fullerton, California 92634.
- <sup>11</sup>Manufactured by Cathodeon, Ltd., Nuffield Road, Cambridge, England CB41TF.
- <sup>12</sup>Manufactured by Infrared Laboratories, Inc., 1165 North Belvedere, Tucson, Arizona 85712.
- <sup>13</sup>General Automation, Inc., Anaheim, California 92805.
- <sup>14</sup>Manufactured by California Computers, Inc., Anaheim, California.
- <sup>15</sup>P. Fisher, W. H. Haak, E. J. Johnson, and A. K. Ramdas, *Proceedings of the Eighth Symposium on the Art of Glass Blowing* (The American Scientific Glass Blowers Society, Wilmington, Delaware, 1963), p. 136.
- <sup>16</sup>Insulating Material Department, General Electric Co., Schenectady, New York.
- <sup>17</sup>J. Gilman, *The Art and Science of Growing Crystals* (Wiley, New York, 1963); R. A. Laudise, *The Growth of Single Crystals* (Prentice-Hall, Englewood Cliffs, New Jersey, 1970); W. D. Lawson and S. Nielsen, *Preparation of Single Crystals* (Butterworths, London, 1960).
- <sup>18</sup>R. L. Aggarwal, P. Fisher, V. Mourzine, and A. K. Ramdas, *Phys. Rev.* **138**, A882 (1965).
- <sup>19</sup>K. Lark-Horovitz, in *Semi-Conducting Materials*, edited by H. K. Henisch (Butterworths, London, 1951), p. 47.
- <sup>20</sup>M. Tannenbaum and A. D. Mills, *J. Electrochem. Soc.* **108**, 171 (1961).
- <sup>21</sup>The neutron irradiations were carried out at the Research Reactor Facility, University of Missouri, Columbia, Mo. through the courtesy of Dr. J. M. Meese. An earlier short account of the excitation spectra of NTD silicon appears in C. Jagannath, Z. W. Grabowski, and A. K. Ramdas, *Solid State Commun.* **29**, 355 (1979).
- <sup>22</sup>The original sample manufactured by Hughes Air Craft was *p* type with a resistivity of 5000  $\Omega$  cm, and a minority lifetime of 1000  $\mu$ sec. It is a float zone, multipassed and pulled in a  $\langle 111 \rangle$  direction.
- <sup>23</sup>T. M. Lifshits and F. Ya. Nad, *Sov. Phys. Dokl.* **10**, 532 (1965) [*Dokl. Akad. Nauk SSSR* **162**, 801 (1965)]; S. M. Kogan and B. I. Sedunov, *Sov. Phys. Solid State* **8**, 1898 (1967) [*Fiz. Tverd. Tela.* **8**, 2382 (1966)].
- <sup>24</sup>P. Fisher and A. K. Ramdas, in *Physics of the Solid State*, edited by S. Balakrishna, M. Krishnamurthi, and B. Ramachandra Rao (Academic, New York, 1969), p. 149.
- <sup>25</sup>W. Kohn and J. M. Luttinger, *Phys. Rev.* **98**, 915 (1955).
- <sup>26</sup>R. A. Faulkner, *Phys. Rev.* **184**, 713 (1969).
- <sup>27</sup>H. Reiss and C. S. Fuller, in *Semiconductors*, edited by N. B. Hannay (Reinhold, New York, 1960), Chap. VI.
- <sup>28</sup>H. F. Wolf, *Silicon Semiconductor Data* (Pergamon, New York, 1969), Chap. III.
- <sup>29</sup>E. M. Pell, in *Solid State Physics in Electronics and Telecommunications*, edited by M. Désirant and J. L. Michiels (Academic, New York, 1960), Vol. 1, p. 261.
- <sup>30</sup>R. M. Chrenko, R. S. McDonald, and E. M. Pell, *Phys. Rev.* **138**, A1775 (1965).
- <sup>31</sup>High-purity float zone silicon manufactured by Dow Corning, Hemlock, Michigan 48626. Resistivity of sample  $\sim 1500$ – $3000 \Omega$  cm.
- <sup>32</sup>G. D. Watkins and F. S. Ham, *Phys. Rev. B* **1**, 4071 (1970).
- <sup>33</sup>T. E. Gilmer, Jr., R. K. Franks, and R. J. Bell, *J. Phys. Chem. Solids* **26**, 1195 (1965).
- <sup>34</sup>Hyperpure silicon sample manufactured by TOPSIL, 105 South Midway Road, Shelter Island, N.Y. 11964. The sample was *n* type with a resistivity of 6000  $\Omega$  cm and a minority carrier lifetime of 2500  $\mu$ sec.
- <sup>35</sup>W. Kaiser, P. H. Keck, and C. F. Lange, *Phys. Rev.* **101**, 1264 (1956).
- <sup>36</sup>W. Kaiser and P. H. Keck, *J. Appl. Phys.* **28**, 882 (1957).
- <sup>37</sup>B. T. Alhburn, Ph.D. thesis (Purdue University, 1969) (unpublished).
- <sup>38</sup>D. Sampson and H. Margenau, *Phys. Rev.* **103**, 879 (1956).
- <sup>39</sup>R. Barrie and K. Nishikawa, *Can. J. Phys.* **41**, 1823 (1963).
- <sup>40</sup>J. D. Jackson, *Classical Electrodynamics* (Wiley, New York, 1962), p. 69.
- <sup>41</sup>See for example, L. D. Landau and E. M. Lifshitz, *Quantum Mechanics, Non-Relativistic Theory* (Pergamon, London, 1958), p. 254.
- <sup>42</sup>D. M. Larsen, *Phys. Rev. B* **8**, 535 (1973).
- <sup>43</sup>W. Baltensperger, *Philos. Mag.* **44**, 1355 (1953).
- <sup>44</sup>K. Colbow, *Can. J. Phys.* **41**, 1801 (1963).
- <sup>45</sup>S. N. Artjemenko, A. A. Kal'fa, S. M. Kogan, and V. I. Sidorov, *Sov. Phys. Semicond.* **8**, 1405 (1975) [*Fiz. Tekh. Poluprovoda* **8**, 2164 (1974)].
- <sup>46</sup>W. Kohn, in *Solid State Physics*, edited by F. Seitz and D. Turnbull (Academic, New York, 1957), Vol. 5, p. 257.
- <sup>47</sup>A. J. R. deKock, in *Handbook on Semiconductors*, edited by S. P. Keller (North-Holland, New York, 1980), Vol. 3.
- <sup>48</sup>See D. S. Billington and J. H. Crawford, *Radiation Damage in Solids* (Princeton University Press, Princeton, New Jersey, 1961).
- <sup>49</sup>Private communication from Dr. J. M. Meese, Research Reactor Facility, University of Missouri, Columbia, Mo., where the irradiations were carried out.
- <sup>50</sup>M. Capizzi, G. A. Thomas, F. DeRosa, R. N. Bhatt, and T. M. Rice, *Solid State Commun.* **31**, 611 (1979).
- <sup>51</sup>E. M. Bykova, T. M. Lifshits, and V. I. Sidorov, *Sov. Phys. Semicond.* **7**, 671 (1973) [*Fiz. Tekh. Poluprovoda* **7**, 986 (1973)].
- <sup>52</sup>Note the lines 4 and 4A in Si(B) reported in Ref. 6 have been resolved into 4, 4B, and 4A at 39.61, 39.68, and 39.92 meV, respectively. The line at 39.68 meV (4B) has been reported by M. S. Skolnick, L. Eaves, R. A. Stradling, J. C. Portal, and S. Askenazy, *Solid State Commun.* **15**, 1403 (1974); the higher resolution in the present measurements ( $0.06 \text{ cm}^{-1}$ ) has resulted in 4B being more clearly resolved.
- <sup>53</sup>Y. Nisida, K. Horii, and K. Muro, *J. Phys. Soc. Jpn.* **29**, 1388 (1970).
- <sup>54</sup>A. Imatake, *J. Phys. Soc. Jpn.* **35**, 164 (1973).
- <sup>55</sup>A. C. Carter, G. P. Carver, R. J. Nicholas, J. C. Portal, and R. A. Stradling, *Solid State Commun.* **24**, 55 (1977).
- <sup>56</sup>K. Jain, S. Lai, and M. V. Klein, *Phys. Rev. B* **13**, 5448 (1976).
- <sup>57</sup>J. Doehler, P. J. Colwell, and S. A. Solin, *Phys. Rev. B* **9**, 636 (1974).